Finite volume scheme for the 1D Maxwell equations with GSTC conditions

Loula Fatima Fezoui, Stéphane Lanteri

Finite volume scheme for the 1D Maxwell equations with GSTC conditions

Loula Fezoui and Stéphane Lanteri

RESEARCH REPORT
N° 9156
Februray 2018
Project-Teams Nachos

ISSN 0249-6399 ISRN INRIA/RR--9156--FR+ENG

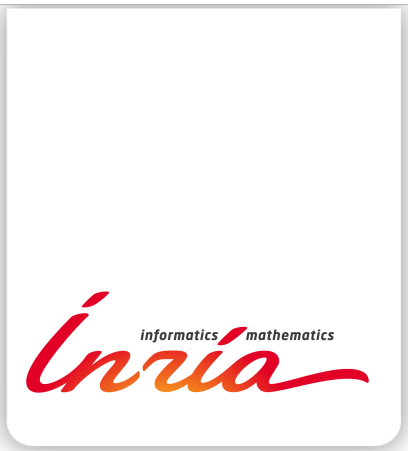

Finite volume scheme for the 1D Maxwell equations with GSTC conditions

Loula Fezoui and Stéphane Lanteri

Project-Teams Nachos

Research Report n° 9156 — Februray 2018 — 14 pages

Abstract: We propose a Finite Volume Time-Domain scheme for the numerical treatment of Generalized Sheet Transition Conditions (GSTC) modeling metasurfaces in the one-dimensional case.

Key-words: Metasurfaces, time-domain Maxwell equations, GSTC conditiuons, finite volume method.

RESEARCH CENTRE
SOPHIA ANTIPOLIS – MÉDITERRANÉE

2004 route des Lucioles - BP 93
06902 Sophia Antipolis Cedex

Schéma volume fini pour les équations de Maxwell 1D couplées aux conditions GSTC

Résumé : On propose un schéma volume fini en domaine temporel pour le traitement numérique des conditions de transfert généralisées modélisant la discontinuité du champ électromagnétique traversant une métasurface dans le cas 1D.

Mots-clés : Métasurfaces, équations de Maxwell en domaine temporel, conditions GSTC, méthode volume fini

1 Introduction

Metasurfaces are artificial devices designed for controlling electromagnetic waves through the surface electric and magnetic susceptibility tensors. Conversely, in some cases, one may deduce these parameters from the surrounding electromagnetic field ([2], [3]). The connection between susceptibility tensors and the electromagnetic field may be given through boundary conditions. Such conditions are called GSTC for **G**eneralized **S**heet **T**ransition **C**onditions and were established in the frequency-domain (see [1] and references therein). Numerical simulations were carried out using finite difference methods first in the frequency-domain (cf. [5]) and then in the time-domain (cf. [4]).

Here, we propose a new finite volume scheme that can handle these unusual boundary conditions. Numerical results are compared to analytical and FDTD solutions.

2 Maxwell equations

Let us consider a metasurface at $z = 0$, parallel to the Ox axis. We choose a TE_y polarisation (ie $\bar{\mathbf{E}} = (0, \bar{E}_y, 0)^\intercal$, $\bar{\mathbf{H}} = (\bar{H}_x, 0, 0)^\intercal$) and assume that fields depend only on z and t variables and that there is no charge or current. Thus Maxwell equations are written as

$$\left\{ \begin{array}{ll} \mu \dfrac{\partial \bar{H}_x}{\partial t} - \dfrac{\partial \bar{E}_y}{\partial z} & = 0 \\ \varepsilon \dfrac{\partial \bar{E}_y}{\partial t} - \dfrac{\partial \bar{H}_x}{\partial z} & = 0 \end{array} \right. \tag{1}$$

We introduce the following change of variables

$$\tau = c_0 t, \quad \varepsilon_r = \frac{\varepsilon}{\varepsilon_0}, \quad \mu_r = \frac{\mu}{\mu_0}, \quad \mathbf{E} = \bar{\mathbf{E}}, \quad \mathbf{H} = c_0 \mu_0 \bar{\mathbf{H}} = Z_0 \bar{\mathbf{H}} \tag{2}$$

where Z_0 is the characteristic impedance of free space. Assuming the medium surrounding the metasurface is the vacuum, (1) becomes

$$\left\{ \begin{array}{ll} \dfrac{\partial H}{\partial \tau} - \dfrac{\partial E}{\partial z} & = 0 \\ \dfrac{\partial E}{\partial \tau} - \dfrac{\partial H}{\partial z} & = 0 \end{array} \right. , \quad E = E_y, \;\; H = H_x \tag{3}$$

We set $I_1 =]-\infty, 0[$, $I_2 =]0, +\infty[$ and add the following initial conditions

$$\left\{ \begin{array}{lll} H_0(z) = H(z,0) & = & \left\{ \begin{array}{ll} g_1(z) & \text{if } z \in I_1 \\ g_2(z) & \text{if } z \in I_2 \end{array} \right. \\ E_0(z) = E(z,0) & = & \left\{ \begin{array}{ll} f_1(z) & \text{if } z \in I_1 \\ f_2(z) & \text{if } z \in I_2 \end{array} \right. \end{array} \right. \tag{4}$$

where f_j and g_j are arbitrary regular functions defined on I_j. We can easily check that the

general solution to (3)-(4) is given by

$$\left\{\begin{array}{rcl} H(z,t) & = & \dfrac{1}{2}\left\{\begin{array}{ll} (g_1-f_1)(z-t)+(f_1+g_1)(z+t) & \text{if } z\in I_1 \\ (g_2-f_2)(z-t)+(f_2+g_2)(z+t) & \text{if } z\in I_2 \end{array}\right. \\ E(z,t) & = & \dfrac{1}{2}\left\{\begin{array}{ll} (f_1-g_1)(z-t)+(f_1+g_1)(z+t) & \text{if } z\in I_1 \\ (f_2-g_2)(z-t)+(f_2+g_2)(z+t) & \text{if } z\in I_2 \end{array}\right. \end{array}\right. \tag{5}$$

3 GSTC conditions

We introduce electric and magnetic surface polarisation fields $\bar{P}$ and $\bar{M}$ and GSTC boundary conditions are written in the time-domain (cf. [5]) as

$$\left\{\begin{array}{rcl} \dfrac{d\bar{P}}{dt} & = & \Delta\bar{H} \\ \dfrac{d\bar{M}}{dt} & = & \dfrac{1}{\mu_0}\Delta\bar{E} \end{array}\right. , \quad \Delta U = U(0^+) - U(0^-) \tag{6}$$

The polarisation fields $\bar{P}$ and $\bar{M}$ are connected to the electric and magnetic fields $\bar{E}$ and $\bar{H}$ through the following equations

$$\left\{\begin{array}{rcl} \bar{P} & = & \varepsilon_0\chi_e\bar{E}_{av} \\ \bar{M} & = & \chi_m\bar{H}_{av} \end{array}\right. , \quad U_{av} = \frac{1}{2}\left(U(0^+)+U(0^-)\right) \tag{7}$$

where χ_e and χ_m are respectively the electric and magnetic surface susceptibility.

We set $P = \bar{P}/\varepsilon_0$ and $M = Z_0\bar{M}$ then (6) becomes

$$\left\{\begin{array}{rcl} \dfrac{dP}{d\tau} & = & \Delta H \\ \dfrac{dM}{d\tau} & = & \Delta E \end{array}\right. \tag{8}$$

with

$$\left\{\begin{array}{rcl} P & = & \chi_e E_{av} \\ M & = & \chi_m H_{av} \end{array}\right. \tag{9}$$

We inject (9) into (8) and we obtain

$$\left\{\begin{array}{l} \Delta H = \dfrac{d}{d\tau}\Big(\chi_e E_{av}\Big) \\ \Delta E = \dfrac{d}{d\tau}\Big(\chi_m H_{av}\Big) \end{array}\right. \tag{10}$$

Inserting (10) in the general solution (5) leads to the first-order differential system

$$\left\{\begin{array}{l} \dfrac{d}{d\tau}\Big\{\chi_e\Big((F_s-G_s)(-\tau)+(F_s+G_s)(\tau)\Big)\Big\} = 2\Big((G_d-F_d)(-\tau)+(F_d+G_d)(\tau)\Big) \\ \dfrac{d}{d\tau}\Big(\chi_m\Big(G_s-F_s)(-\tau)+(F_s+G_s)(\tau)\Big)\Big\} = 2\Big((F_d-G_d)(-\tau)+(F_d+G_d)(\tau)\Big) \end{array}\right. \tag{11}$$

with

$$F_s = f_1 + f_2, \quad G_s = g_1 + g_2, \quad F_d = f_2 - f_1, \quad G_d = g_2 - g_1 \tag{12}$$

If we assume that χ_e and χ_m are time-independent, conditions (10) are written as

$$\begin{cases} \Delta H = \chi_e \dfrac{d}{d\tau}\Big(E_{av}\Big) \\ \\ \Delta E = \chi_m \dfrac{d}{d\tau}\Big(H_{av}\Big) \end{cases} \tag{13}$$

and the differential system (11) becomes

$$\begin{cases} \chi_e \dfrac{d}{d\tau}\Big\{(F_s - G_s)(-\tau) + (F_s + G_s)(\tau)\Big\} = 2\Big((G_d - F_d)(-\tau) + (F_d + G_d)(\tau)\Big) \\ \\ \chi_m \dfrac{d}{d\tau}\Big\{(G_s - F_s)(-\tau) + (F_s + G_s)(\tau)\Big\} = 2\Big((F_d - G_d)(-\tau) + (F_d + G_d)(\tau)\Big) \end{cases} \tag{14}$$

4 The Finite Volume Time-Domain method (FVTD)

We write Maxwell equations (3) in the conservative formulation

$$\frac{\partial \mathbf{Q}}{\partial \tau} - \left(\frac{\partial \mathbf{F}}{\partial z}\right)(\mathbf{Q}) = 0 \tag{15}$$

with

$$\mathbf{Q} = (H, E)^\intercal, \quad \mathbf{F}(\mathbf{Q}) = (E, H)^\intercal \tag{16}$$

Let $z_j = (j-1)\Delta z$ and $\mathcal{C}_j = [z_j, z_{j+1}]$. Integrating (15) on each $\mathcal{C}_j$ element gives

$$\int_{\mathcal{C}_j} \frac{\partial \mathbf{Q}}{\partial \tau} d\tau = \int_{\mathcal{C}_j} \frac{\partial \mathbf{F}}{\partial z} dz = \Big[\mathbf{F}\Big]_{z_j}^{z_{j+1}} \tag{17}$$

In finite volume methods, the approximate solution is independent of space variables in each C_j element, therefore the value $\mathbf{Q}_j = \mathbf{Q}(z_j)$ is not unique. We usually introduce a numerical function Φ (known as the *numerical flux function* in fluid mechanics) and we write

$$\mathbf{F}(\mathbf{Q}_j) \approx \Phi\left(\mathbf{Q}_{j-1}, \mathbf{Q}_j\right) \tag{18}$$

We inject (18) in (17) and the finite volume scheme becomes

$$\frac{d\mathbf{Q}_j}{d\tau} = \frac{1}{\Delta z}\Big[\Phi\left(\mathbf{Q}_j, \mathbf{Q}_{j+1}\right)(\tau) - \Phi\left(\mathbf{Q}_{j-1}, \mathbf{Q}_j\right)(\tau)\Big] \tag{19}$$

The function Φ is not unique. We choose the central average flux defined by

$$\Phi(U, V) = \frac{\mathbf{F}(U) + \mathbf{F}(V)}{2} \tag{20}$$

and (19) becomes

$$\frac{d\mathbf{Q}_j}{d\tau} = \frac{1}{2\Delta z}\Big[\mathbf{F}\left(\mathbf{Q}_{j+1}\right) - \mathbf{F}\left(\mathbf{Q}_{j-1}\right)\Big] \tag{21}$$

or in terms of E and H

$$\left\{\begin{array}{rcl} \dfrac{dE_j}{d\tau} & = & \dfrac{1}{2\Delta z}\left(H_{j+1}-H_{j-1}\right) \\ \dfrac{dH_j}{d\tau} & = & \dfrac{1}{2\Delta z}\left(E_{j+1}-E_{j-1}\right)(\tau) \end{array}\right. \tag{22}$$

The approximate solution being constant in each $\mathcal{C}_j$ element, the metasurface must be located at the interface of two adjacents elements named $\mathcal{C}_\kappa$ and $\mathcal{C}_{\kappa-1}$, where κ is the index of the point $z=0$. We use a leap-frog scheme for time integration and (22) becomes

$$\left\{\begin{array}{rcl} E_j^n & = & E_j^{n-1} + \nu\left(H_{j+1}^{n-\frac{1}{2}} - H_{j-1}^{n-\frac{1}{2}}\right) \\ H_j^{n+\frac{1}{2}} & = & H_j^{n-\frac{1}{2}} + \nu\left(E_{j+1}^{n} - E_{j-1}^{n}\right) \end{array}\right. , \qquad \nu = \frac{\Delta\tau}{2\Delta z} \tag{23}$$

We use (23) to compute (E_j, H_j) for each j except for $j=\kappa-1$ and $j=\kappa$ in which case we write

$$\left\{\begin{array}{rcl} E_{\kappa-1}^n & = E_{\kappa-1}^{n-1} - \nu\left(H_{\kappa-1}^{n-\frac{1}{2}} + H_{\kappa-2}^{n-\frac{1}{2}}\right) + \dfrac{\Delta\tau}{\Delta z}H^{n-\frac{1}{2}}(0^-) \\ E_{\kappa}^n & = E_{\kappa}^{n-1} + \nu\left(H_{\kappa+1}^{n-\frac{1}{2}} + H_{\kappa}^{n-\frac{1}{2}}\right) - \dfrac{\Delta\tau}{\Delta z}H^{n-\frac{1}{2}}(0^+) \\ H_{\kappa-1}^{n+\frac{1}{2}} & = H_{\kappa-1}^{n-\frac{1}{2}} - \nu\left(E_{\kappa-1}^{n} + E_{\kappa-2}^{n}\right) + \dfrac{\Delta\tau}{\Delta z}E^{n}(0^-) \\ H_{\kappa}^{n+\frac{1}{2}} & = H_{\kappa}^{n-\frac{1}{2}} + \nu\left(E_{\kappa+1}^{n} + E_{\kappa}^{n}\right) - \dfrac{\Delta\tau}{\Delta z}E^{n}(0^+) \end{array}\right. \tag{24}$$

We integrate (13) using the same leap-frog scheme and obtain

$$\left\{\begin{array}{rcl} H^{n-\frac{1}{2}}(0^+) - H^{n-\frac{1}{2}}(0^-) & = & \dfrac{\chi_e}{\Delta\tau}\left[E_{av}^n - E_{av}^{n-1}\right] \\ E^n(0^+) - E^n(0^-) & = & \dfrac{\chi_m}{\Delta\tau}\left[H_{av}^{n+\frac{1}{2}} - H_{av}^{n-\frac{1}{2}}\right] \end{array}\right. \tag{25}$$

with

$$H_{av}^{n+\frac{1}{2}} = \frac{1}{2}\left[H^{n+\frac{1}{2}}(0^+) + H^{n+\frac{1}{2}}(0^-)\right], \quad E_{av}^n = \frac{1}{2}\left[E^n(0^+) + E^n(0^-)\right] \tag{26}$$

We inject (26) into (25) and obtain

$$\left\{\begin{array}{rcl} H^{n-\frac{1}{2}}(0^+) & = & H^{n-\frac{1}{2}}(0^-) + \dfrac{\chi_e}{2\Delta\tau}\left(E^n(0^+) - E^{n-1}(0^+) + E^n(0^-) - E^{n-1}(0^-)\right) \\ E^n(0^+) & = & E^n(0^-) + \dfrac{\chi_m}{2\Delta\tau}\left(H^{n+\frac{1}{2}}(0^+) - H^{n-\frac{1}{2}}(0^+) + H^{n+\frac{1}{2}}(0^-) - H^{n-\frac{1}{2}}(0^-)\right) \end{array}\right. \tag{27}$$

(27) is an underdetermined linear system with too many unknowns so we decide to keep $E^n(0^+)$ and $H^{n-\frac{1}{2}}(0^+)$ as unknowns. Setting $U(0^-) = U_{\kappa-1}, U(0^+) = U_\kappa$ in the R.H.S. of (27) leads to

$$\left\{\begin{array}{rcl} H^{n-\frac{1}{2}}(0^+) & = & H_{\kappa-1}^{n-\frac{1}{2}} + \dfrac{\chi_e}{2\Delta\tau}\left(E_{\kappa}^n - E_{\kappa}^{n-1} + E_{\kappa-1}^n - E_{\kappa-1}^{n-1}\right) \\ E^n(0^+) & = & E_{\kappa-1}^n + \dfrac{\chi_m}{2\Delta\tau}\left(H_{\kappa}^{n+\frac{1}{2}} - H_{\kappa}^{n-\frac{1}{2}} + H_{\kappa-1}^{n+\frac{1}{2}} - H_{\kappa-1}^{n-\frac{1}{2}}\right) \end{array}\right. \tag{28}$$

We inject (28) into (24) and set $U(0^-) = U_{\kappa-1}$ in the R.H.S. of (24) and obtain

$$\left\{\begin{array}{lcll} E^n_{\kappa-1} & = & E^{n-1}_{\kappa-1} + \nu\left(H^{n-\frac{1}{2}}_{\kappa-1} - H^{n-\frac{1}{2}}_{\kappa-2}\right) & \\ E^n_{\kappa} & = & E^{n-1}_{\kappa} + \nu\left(H^{n-\frac{1}{2}}_{\kappa+1} - 2H^{n-\frac{1}{2}}_{\kappa-1} + H^{n-\frac{1}{2}}_{\kappa}\right) & - \quad \mathcal{C}_e\left(E^n_{\kappa} - E^{n-1}_{\kappa} + E^n_{\kappa-1} - E^{n-1}_{\kappa-1}\right) \\ H^{n+\frac{1}{2}}_{\kappa-1} & = & H^{n-\frac{1}{2}}_{\kappa-1} + \nu\left(E^n_{\kappa-1} - E^n_{\kappa-2}\right) & \\ H^{n+\frac{1}{2}}_{\kappa} & = & H^{n-\frac{1}{2}}_{\kappa} + \nu\left(E^n_{\kappa+1} - 2E^n_{\kappa-1} + E^n_{\kappa}\right) & - \quad \mathcal{C}_m\left(H^{n+\frac{1}{2}}_{\kappa} - H^{n-\frac{1}{2}}_{\kappa} + H^{n+\frac{1}{2}}_{\kappa-1} - H^{n-\frac{1}{2}}_{\kappa-1}\right) \end{array}\right.$$

After regrouping terms in the second and fourth equations the scheme becomes (for $j = \kappa$)

$$\left\{\begin{array}{lcll} \mathcal{A}_e E^n_{\kappa} & = & \mathcal{A}_e E^{n-1}_{\kappa} + \nu\left(H^{n-\frac{1}{2}}_{\kappa+1} - 2H^{n-\frac{1}{2}}_{\kappa-1} + H^{n-\frac{1}{2}}_{\kappa}\right) & - \quad \mathcal{C}_e\left(E^n_{\kappa-1} - E^{n-1}_{\kappa-1}\right) \\ \mathcal{A}_m H^{n+\frac{1}{2}}_{\kappa} & = & \mathcal{A}_m H^{n-\frac{1}{2}}_{\kappa} + \nu\left(E^n_{\kappa+1} - 2E^n_{\kappa-1} + E^n_{\kappa}\right) & - \quad \mathcal{C}_m\left(H^{n+\frac{1}{2}}_{\kappa-1} - H^{n-\frac{1}{2}}_{\kappa-1}\right) \end{array}\right. \tag{29}$$

with

$$\mathcal{C}_p = \frac{\chi_p}{2\Delta z}, \quad \mathcal{A}_p = 1 + \mathcal{C}_p, \qquad p = e\ ,\ m \tag{30}$$

5 Numerical Experiments

5.1 Propagation of a gaussian pulse

Let us study the propagation of a gaussian pulse defined at $\tau = 0$ by

$$\left\{\begin{array}{l} f_1(z) = e^{-a(z-z_0)^2} \\ g_1(z) = -f_1(z) \end{array}\right. , \quad a > 0, \quad z_0 \in I_1 \tag{31}$$

We consider two cases

(a) $\chi_e = \chi_m = 0$

(b) $\chi_e = \chi_m = \dfrac{2}{a}$

We solve the system (14) and find respectively

$$(a) \quad f_2 \equiv f_1, \quad g_2 \equiv g_1 \tag{32}$$

$$(b) \left\{\begin{array}{l} f_2(z) = \sqrt{a\pi}\, e^{\frac{a(1+4(z-z_0))}{4}}\left(1 - \mathrm{erf}\left(\frac{\sqrt{a}(1+2(z-z_0))}{2}\right)\right) - f_1(z) \\ g_2(z) = -f_2(z), \qquad \text{with} \quad \mathrm{erf}(x) = \dfrac{2}{\sqrt{\pi}}\int e^{-x^2} dx \end{array}\right. \tag{33}$$

We use (5) to compute the exact electric field and find respectively

$$(a) \quad E(z,\tau) = e^{-a(z-z_0-\tau)^2}, \quad \forall\,(z,\tau), \tag{34}$$

$$(b)\quad E(z,\tau)=\begin{cases} e^{-a(z-z_0-\tau)^2}, & \text{if } z\in I_1 \\ \sqrt{a\pi}e^{\frac{a(1+4(z-z_0-\tau))}{4}}\left(1-\operatorname{erf}\left(\frac{\sqrt{a}(1+2(z-z_0-\tau))}{2}\right)\right)-e^{-a(z-z_0-\tau)^2}, & \text{if } z\in I_2 \end{cases} \tag{35}$$

We set $\chi_e = 0.5$, $z_0 = -1.5$, $I_1 \cup I_2 =]-3,3[$ and $\Delta z = 1/100$ and we plot in Figure 1 the exact solution (35) and the numerical results using the finite volume (23)-(29) and the FDTD schemes (see Annex 1 eqs. 40)-(44)). We may observe that the approximate solutions compare well with each other as well as with the analytical solution.

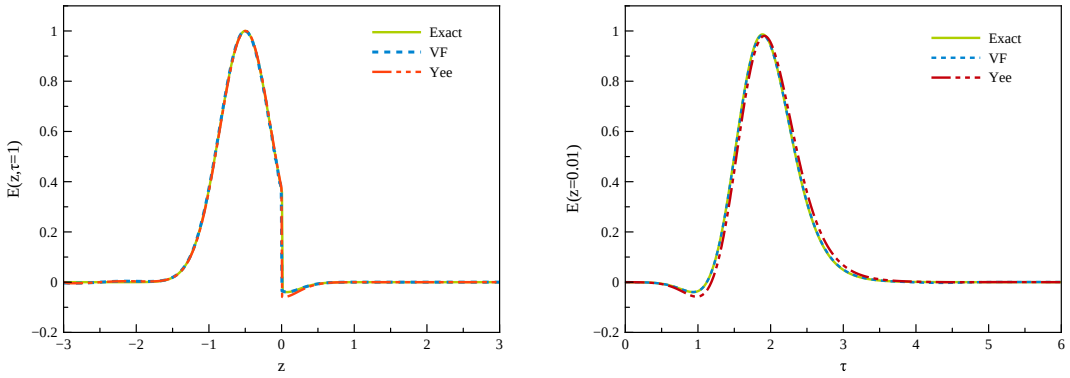

Figure 1: $E(z,\tau=1)$ (left), $E(z=0.01,\tau)$ (right)

To quantify the accuracy of the numerical solutions, we compute the global error at $\tau_n = n\Delta\tau$ using the discrete L^2 norm

$$\sqrt{\sum_j \Delta z\left((E_j^n - E^{\text{exact}}(z_j,\tau_n))^2(H_j^n - H^{\text{exact}}(z_j,\tau_n))^2\right)} \tag{36}$$

Figure 2 shows the evolution over time of error (36) in case (a) (on the left) and in case (b) (on the right). In both cases, as expected, the error decreases with smaller Δz (ie with more refined grids).

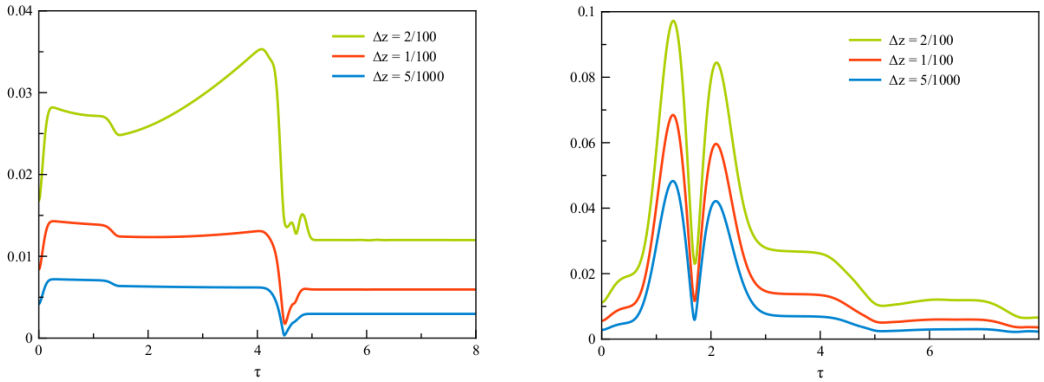

Figure 2: FVTD: L^2 error without (left) and with GSTC (right)

To determine to what extent numerical solutions satisfy GSTC conditions, we compute the following error function

$$\max\left(\left|[E^n(0)] - \frac{\chi_m}{\Delta\tau}\left(H_{av}^{n+\frac{1}{2}} - H_{av}^{n-\frac{1}{2}}\right)\right|, \left|[H^{n-\frac{1}{2}}(0)] - \frac{\chi_e}{\Delta\tau}\left(E_{av}^{n} - E_{av}^{n-1}\right)\right|\right) \tag{37}$$

with $[U(0)] = U(0^+) - U(0^-)$.

Figure 3 shows the evolution over time of error (37) on different grids. We can see that this error is smaller that the global error (36), which means that the GSTC conditions are better resolved than the Maxwell equations.

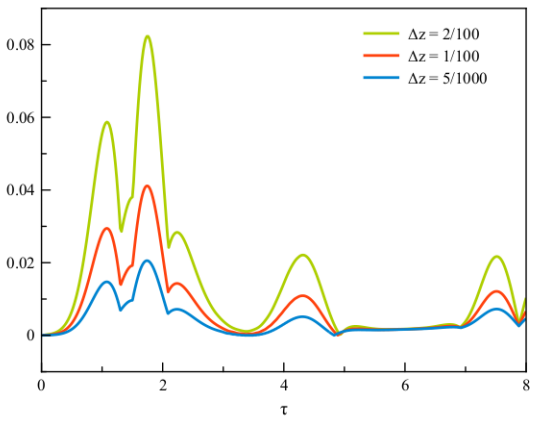

Figure 3: FVTD: error in GSTC conditions

5.2 Metallic cavity

We look for frequency waves in $[-a, a]$ which satisfy the GSTC conditions (13) at $z = 0$ and the perfect metallic condition at $z = \pm a$. Such waves exist and are given by

$$\begin{aligned} E(z,t) &= \begin{cases} \sin(k(z+a))\sin(\omega t), & z < 0 \\ \sin(k(z-a))\sin(\omega t), & z > 0 \end{cases} \\ H(z,t) &= \begin{cases} -\cos(k(z+a))\cos(\omega t), & z < 0 \\ -\cos(k(z-a))\cos(\omega t), & z > 0 \end{cases} \end{aligned} \tag{38}$$

with

$$\chi_e = 0, \quad \chi_m = -\frac{2}{k}\tan(ka), \quad k = \omega = n\pi, \quad n \in \mathbb{N} \tag{39}$$

Remark 1. *The unusual form of the dispersion relation $k = \omega$ stems from the change of variables described in section 2.*

We choose $k = 2\pi$ (which corresponds to a frequency of 0.3 GHz and a wavelength of 1 m) and $\chi_m = 0.02$ ($a \approx 1.5$). Figure 4 shows the analytical electric field and numerical results obtained with FVTD and FDTD schemes.

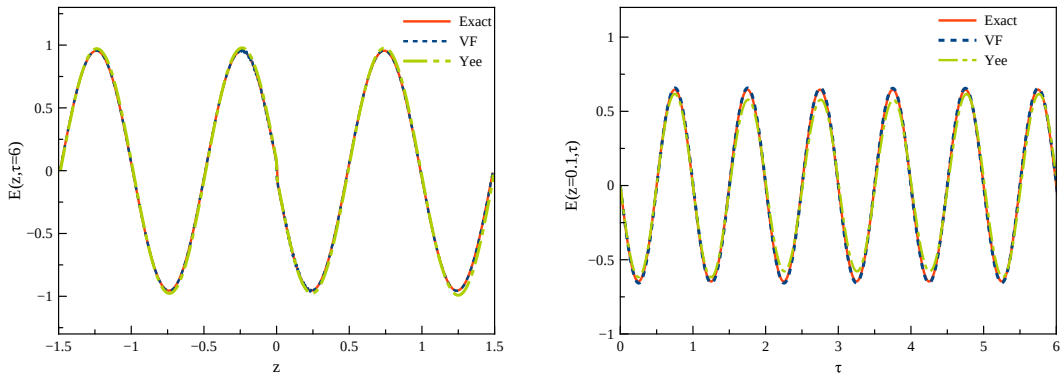

Figure 4: $E(z, \tau = 6)$ (left) and $E(z = 0.1, \tau)$ (right)

We can see that computed and exact solutions compare relatively well with each other, however comparison with the exact solution favours the FVTD solution. Figure 5 shows the (36) and (13) errors on different grids. We notice that while the former error decreases with Δz for both schemes, the latter grows with τ for the FDTD scheme and decreases for the FVTD scheme. However we can see on the right side of Figure 5 that error (37) is much the same for both schemes.

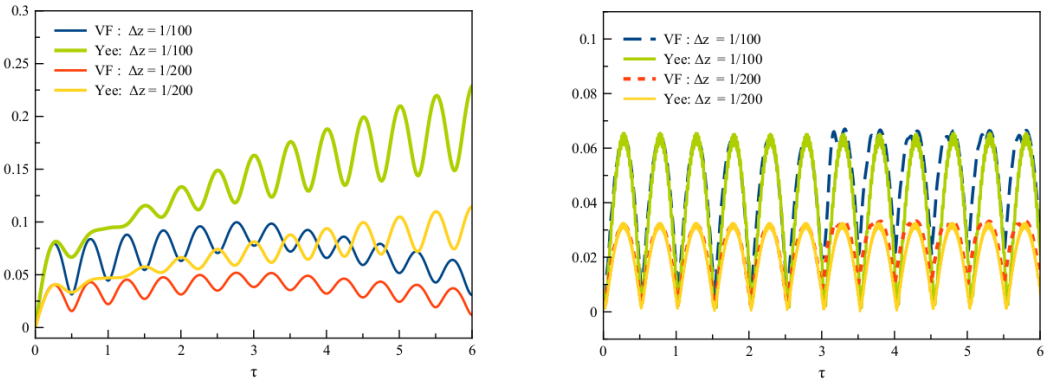

Figure 5: L^2 error in solutions (left) and error in GSTC conditions (right)

References

[1] E.F. Kuester, M.A. Mohamed, M. Piket-May, C.L. Holloway *"Averaged Transition Conditions for Electromagnetic Fields at a Metafilm"*, IEEE Trans. Antennas Propag., vol. 51, no. 10, 2003.

[2] C.L. Holloway, A. Dienstfrey, E.F. Kuester, J. O'Hara, A.K. Azad, A.J. Taylor, *'A discussion on the interpretaion and characterization of metafilms/metasurfaces: the two-dimensional equivalent of metamaterials"*, IEEE Trans. Antennas Propag., vol. 3, no. 2, 2009.

[3] K. Achouri, M.-A. salem, C. Caloz, *"General Metasurface Synthesis based on Susceptibility Tensors"*, IEEE. Trans. Antennas Propag., vol. 63, no. 7, 2015.

[4] Y. Vahabzadeh, K. Achouri, C. Caloz, *"Simulation of Metasurfaces in Finite Difference Techniques"*, Arxiv 1602.04086v1, Feb 2016.

[5] Y. Vahabzadeh, N. Chamanara, C. Caloz, *"Space-Time Varying Metasurfaces Simulation in Finite Difference Time Domain"*, Arxiv 1702.08760v1, Jan 2017.

[6] K. Yee, *"Numerical solution of initial boundary value problems invoking Maxwell's equations in isotropic media"*, IEEE. Trans. Antennas Propag., vol. 14, no. 7, 1966.

1 The finite-difference time-domain method (FDTD)

Let us briefly recall the FDTD scheme described in [5]. We introduce the following notations

$$z_j = (j-1)\Delta z, \quad \tau_n = n\Delta\tau, \quad \upsilon = \frac{\Delta\tau}{\Delta z},$$

$$E_j^n = E(z_j, n\Delta\tau), \quad H_j^{n+\frac{1}{2}} = H(z_{j+\frac{1}{2}}, \tau^{n+\frac{1}{2}})$$

Applied to (3), the Yee scheme [6] is written as

$$\left\{ \begin{array}{lcl} E_j^n & = & E_j^{n-1} + \upsilon \left(H_j^{n-\frac{1}{2}} - H_{j-1}^{n-\frac{1}{2}} \right) \\ H_j^{n+\frac{1}{2}} & = & H_j^{n-\frac{1}{2}} + \upsilon \left(E_{j+1}^n - E_j^n \right) \end{array} \right. , \tag{40}$$

In (40) the electric field is computed at the nodes z_j and the magnetic H at $z_j + \frac{\Delta z}{2}$ and since these fields are discontinuous along the metasurface, the authors of [5] suggest to place the metasurface in $](\kappa + \frac{1}{2})\Delta z,\ (\kappa+1)\Delta z[$, with κ chosen so that z_κ and $z_{\kappa+\frac{1}{2}}$ are on the left of the metasurface and $z_{\kappa+1}$ is on the right (Figure 6).

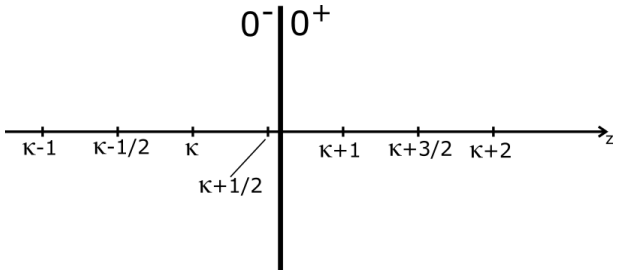

Figure 6: Metasurface at $z = 0$

The usual Yee scheme is used to compute all values E_j and H_j, except $E_{\kappa+1}$ and H_κ for which we write

$$\left\{ \begin{array}{lcl} E_{\kappa+1}^n & = & E_{\kappa+1}^{n-1} + \upsilon \left(H_{\kappa+1}^{n-\frac{1}{2}} - H^{n-\frac{1}{2}}(0^+) \right) \\ H_\kappa^{n+\frac{1}{2}} & = & H_\kappa^{n-\frac{1}{2}} + \upsilon \left(E^n(0^-) - E_\kappa^n \right) \end{array} \right. \tag{41}$$

The values $H^{n-\frac{1}{2}}(0^+)$ and $E^n(0^-)$ are computed using the boundary conditions (13) discretized here as

$$\left\{ \begin{array}{lcl} E^n(0^-) & = & E_{\kappa+1}^n - \frac{\chi_m}{2\Delta\tau} \left(H_\kappa^{n+\frac{1}{2}} - H_\kappa^{n-\frac{1}{2}} - H^{n+\frac{1}{2}}(0^+) + H^{n-\frac{1}{2}}(0^+) \right) \\ H^{n-\frac{1}{2}}(0^+) & = & H_\kappa^{n-\frac{1}{2}} + \frac{\chi_e}{2\Delta\tau} \left(E_{\kappa+1}^n - E_{\kappa+1}^{n-1} + E^n(0^-) - E^{n-1}(0^-) \right) \end{array} \right. \tag{42}$$

We inject (42) into (41) and obtain

$$\left\{\begin{array}{rcl} E_{\kappa+1}^{n} & = & E_{\kappa+1}^{n-1} + \upsilon\left(H_{\kappa+1}^{n-\frac{1}{2}} - H_{\kappa}^{n-\frac{1}{2}}\right) \\ & - & \frac{\chi_e}{2\Delta z}\Big(E_{\kappa+1}^{n} - E_{\kappa+1}^{n-1} - E^{n}(0^-) + E^{n-1}(0^-)\Big) \\ H_{\kappa}^{n+\frac{1}{2}} & = & H_{\kappa}^{n-\frac{1}{2}} + \upsilon\Big(E_{\kappa+1}^{n} - E_{\kappa}^{n}\Big) \\ & - & \frac{\chi_m}{2\Delta z}\left(H_{\kappa}^{n+\frac{1}{2}} - H_{\kappa}^{n-\frac{1}{2}} - H^{n+\frac{1}{2}}(0^+) + H^{n-\frac{1}{2}}(0^+)\right) \end{array}\right. \tag{43}$$

We set $H(0^+) = H_{\kappa+1}$ and $E(0^-) = E_{\kappa}$. After regrouping terms, the scheme (43) becomes

$$\left\{\begin{array}{lcl} A_e E_{\kappa+1}^{n} = A_e E_{\kappa+1}^{n-1} & + & \upsilon\left(H_{\kappa+1}^{n-\frac{1}{2}} - H_{\kappa}^{n-\frac{1}{2}}\right) - C_e\Big(E_{\kappa}^{n} - E_{\kappa}^{n-1}\Big) \\ A_m H_{\kappa}^{n+\frac{1}{2}} = A_m H_{\kappa}^{n-\frac{1}{2}} & + & \upsilon\Big(E_{\kappa+1}^{n} - E_{\kappa}^{n}\Big) - C_m\left(H_{\kappa+1}^{n+\frac{1}{2}} - H_{\kappa+1}^{n-\frac{1}{2}}\right) \end{array}\right. \tag{44}$$

where

$$C_p = \frac{\chi_p}{2\Delta z}, \quad A_p = 1 + C_p, \qquad p = e\,, m$$

Remark 2. *We note that if $\chi_e = 0$ and/or $\chi_m = 0$ then $\{C_e = 0, A_e = 1\}$ and/or $\{C_m = 0, A_m = 1\}$ and (44) reduces to the classical Yee scheme (40) for $j = \kappa + 1$ and/or $j = \kappa$.*

Remark 3. *The scheme (44) differs slightly from that described in [5] since we found that the constant $B_p = 1 - C_p$ is in fact equal to A_p.*

Contents

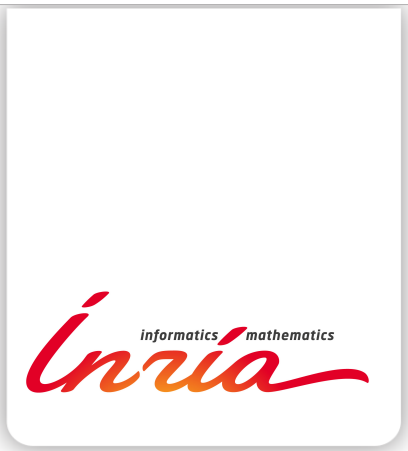

RESEARCH CENTRE
SOPHIA ANTIPOLIS – MÉDITERRANÉE

2004 route des Lucioles - BP 93
06902 Sophia Antipolis Cedex

Publisher
Inria
Domaine de Voluceau - Rocquencourt
BP 105 - 78153 Le Chesnay Cedex
inria.fr

ISSN 0249-6399